Distributed Measurement of Intense Magnetic Fields by Means of Optical Fibers

L. Palmieri[1] **and A. Galtarossa**[1, 2]

[1]Department of Information Engineering, University of Padova, Padova, Italy
[2]IIUSE, Southeast University, Nanjing, China

Abstract— A novel class of distributed fiber optic sensors for the measurement of intense magnetic fields has been recently introduced. The sensors are based on Faraday rotation of polarization and on the distributed polarization measurement of the Rayleigh backscattered light. This paper reviews the current results showing how the technique can be used to map both intensity and direction of strong magnetic field in the area spanned by the optical fiber, with spatial resolution in the order of centimeters.

1. INTRODUCTION

Optical fiber sensors (OFS) are finding wide and successful applications in the monitoring of several structures as diverse as civil buildings, natural sites, energy plants and mechanical components [1]. OFSs offer two main advantages over electro-mechanical sensors; namely, they enable distributed, or quasi-distributed, monitoring and they are intrinsically immune to electromagnetic interference. In particular, the possibility of implementing distributed sensors is an unique feature of OFSs, unparalleled by any other technology, and already successfully exploited in the monitoring of temperature, strain and vibration [1].

The measurement of magnetic fields, based on Faraday rotation of polarization, has been one of the earliest application of OFS [2, 3]. Nonetheless, all magnetic-field OFS developed so far are point sensors, being able to measure the magnetic field only at a specific location. Recently, however, a new distributed optical fiber sensors (DOFS) able to measure the spatial variation of magnetic field along the fiber has been introduced [4–7]. This novel sensor is based on the measurement of the state of polarization (SOP) of the light backscattered by the fiber, as a function of the scattering position, and on the variation of such SOP as a consequence of Faraday rotation. For the sake of completeness, we remark that an early attempt to perform a similar distributed measurement was made by Ross in 1981 [8]. In that case, however, the system was able only to locate the point along the fiber where the magnetic field was varying. More recently, other approaches have been proposed, but the retrieved information about Faraday rotation is not complete [9, 10]. Differently, in the new technique described here the variation of the magnetic field over the whole length of the fiber is completely determined. Tests have been performed using standard telecom fibers, over lengths ranging from few tens of meters to about hundred meters. The reported limit of detection is 100 mT, with a spatial resolution of few centimeters. The measurement uncertainty is about 7%. This paper reviews the main results achieved so far.

2. MEASUREMENT PRINCIPLE

In a non-ideal single-mode optical fiber the polarization of light is not preserved during propagation, but it is changed by almost any kind of perturbation acting along the fiber [11]. Therefore, if we were able to measure that polarization along the fiber, we could retrieve information about those perturbations, and hence about the environment surrounding the fiber. Of course, a direct measurement of the light propagating in the fiber is not practicable, especially over lengths of several tens of meters and beyond. Nonetheless, we can measure the polarization of the Rayleigh backscattered light, and try to infer local information along the fiber. This is the basic idea behind polarization distributed measurements as originally proposed by Rogers [12].

This principle can be used also to measure the magnetic field acting along the fiber through Faraday rotation; there are however two main difficulties. Actually, the backscattered SOP does not directly provide information on the local Faraday rotation, but rather it is the accumulated effect of forward propagation up to a specific point in the fiber, Rayleigh scattering and subsequent back-propagation to the fiber input. Furthermore, the SOP in an optical fiber is not affected only by magnetic field, but also by other perturbations like bending, twist, anisotropy, geometrical asymmetries, etc., which are well known to impair the effectiveness of standard magnetic field

OFS [3]. Therefore, the variation of the backscattered SOP as a function of the scattering position is quite a complex cumulative vectorial function of all perturbations acting along the fiber, where the local information about Faraday rotation is not directly accessible. This difficulty has been however recently overcome by means of an accurate theoretical model, which has enabled the solution of the inverse scattering problem [4].

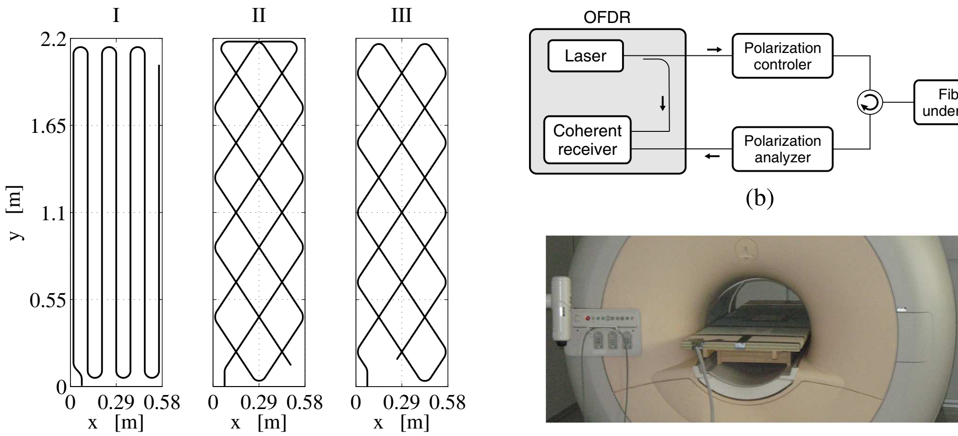

(a) (c)

Figure 1: (a) Paths of the three fibers in sensor A. (b) Schematic of the POFDR setup. (c) Picture of sensor arrangement.

A detailed mathematical description of the measurement procedure would be out of scope, therefore here we report only the main steps of the analysis needed to retrieve the local information; the interested reader may find the complete treatment in the literature [4]. The first step is to measure the 3-dimensional unit Stokes vector, $\mathbf{s}_B(z)$, of the backscattered light as a function of the scattering position, z, for at least 2 different input SOPs. This task can be accomplished by using any polarization sensitive reflectometer, either in the time domain (POTDR), or in the frequency domain (POFDR) [13]. Once the SOPs have been measured, we have to calculate the vector $\boldsymbol{\beta}_B(z)$ such that $d\mathbf{s}_B/dz = \boldsymbol{\beta}_B \times \mathbf{s}_B$. This operation can be solved with the so called Mueller matrix method developed in the framework of polarization mode dispersion measurements [14]. Afterwords, the vector $\boldsymbol{\beta}_B(z)$ is used to numerically solve the differential equation $d\mathbf{B}/dz = (\boldsymbol{\beta}_B/2) \times \mathbf{B}$ with $\mathbf{B}(0) = \mathbf{I}$, where it can be shown that $\mathbf{B}(z)$ is the 3×3 Mueller matrix representing (in a proper reference frame) the backward propagation from the scattering point to the fiber input [4]. Finally, we calculate the vector

$$\boldsymbol{\beta}(z) = \left(\beta_1(z)\,, \beta_2(z)\,, \eta(z)\right)^T = \frac{1}{2}\mathbf{B}^T(z)\boldsymbol{\beta}_B(z)\,, \tag{1}$$

where ^{T} means transposition, and the first two components, β_1 and β_2, summarize the local effects of all perturbations except Faraday rotation, which affects only the third component $\eta(z)$. This net separation enables the distributed measurement of magnetic field along the fiber, and it is due to the non-reciprocal nature of Faraday rotation, which makes it intimately different from all other sources of perturbation [15]. More specifically, the third component of $\boldsymbol{\beta}(z)$ can be expressed as

$$\eta(z) = 2\,V\,B(z)\cos\psi(z), \tag{2}$$

where $B(z)$ is the amplitude of the magnetic induction, $\psi(z)$ is the angle subtended by the magnetic induction and the direction of forward propagation of light, and V is the Verdet constant, which for silica fibers is about $1.43/\lambda^2_{\mu\text{m}}$ (rad/T)/m, so at 1550 nm we have $V \simeq 0.60$ (rad/T)/m [16].

Exploiting the above method and the relationship (2) it is then possible to measure the component of the magnetic field parallel to the fiber axis as a function of the position along the fiber. As shown below, exploiting a proper fiber layout it is also possible to measure more than 1 spatial component of the magnetic field, enabling the making 2- or 3-dimensional vectorial maps. Note, however, that owing to the small value of the Verdet constant and to the distributed nature of the sensor, the proposed sensor is most suited to high intensity fields.

3. 2D VECTORIAL MAPPING OF MAGNETIC FIELD

A first example of application is a sensor, hereinafter "sensor A", to make 2-dimensional vectorial maps of the magnetic field in the area spanned by the fiber. The idea is to deploy the fiber on a mesh so that at each crossing the magnetic field is measured along two directions, enabling the 2-dimensional vectorial mapping [5]. Specifically, 3 standard G.652 fibers have been deployed on wooden boards along the paths shown in Fig. 1(a); the boards were then stacked to form the sought fiber mesh. We used three separate fibers because the range of the measurement setup is limited to 30 m.

The polarization of the backscattered light, $\mathbf{s}_B(z)$, has been measured with a polarization sensitive OFDR, schematically represented in Fig. 1(b). The polarization controller in the forward path allows to change in the input SOP, whereas the polarization analyzer in the backward path allows to calculate $\mathbf{s}_B(z)$. Measurements were performed in a bandwidth of about 40 nm around 1550 nm. Note that while this bandwidth can nominally enable a sub-millimeter spatial resolution, when it comes to SOP measurements further SNR enhancement is required, which is achieved by proper spatial filtering. As a result, the spatial resolution is increased to about 2 cm. Owing to the small value of the Verdet constant in silica, the sensor has been tested exploiting the high magnetic field of a magnetic resonance imaging (MRI) scanner for medical application, which achieved 1.5 T in the imaging area (see Fig. 1(c)).

Figure 2(a) shows the three components of the vector $\boldsymbol{\beta}(z)$ defined in (1) and measured along the fiber of path I (see Fig. 1(a)). The difference between the first two components and the third one is evident. While $\beta_1(z)$ and $\beta_2(z)$ are related to the reciprocal effects, such as anisotropy, bending, twist, etc., and hence vary randomly as a function of z, the third component $\eta(z)$ is affected only to Faraday rotation, and therefore it has markedly ordered behavior. Specifically, up to about 7 m in the fiber η is almost zero, meaning that the Faraday rotation is negligible as it should be, since this is the portion of the fiber that lays outside the MRI and links the sensor to the POFDR. Beyond that distance, the fiber enters the MRI and the effects of the magnetic field become clear. The periodic changes in sign of $\eta(z)$ are actually related to the periodic changes in direction of the fiber with respect to the magnetic field, which make the factor $\cos\psi(z)$ in (2) change its sign accordingly. The value of the magnetic field component along the fiber axis can then be readily calculated exploiting (2), and the results for each of the three fibers are good agreement with the nominal peak value of 1.5 T. By merging the measurements taken on each fiber separately it is then possible to build the 2-dimensional vector map shown in Fig. 2(b). Each arrow indicates modulus and direction of the magnetic field component parallel to the sensor plane, evaluated at each of the more than 100 crossing points of the fiber mesh.

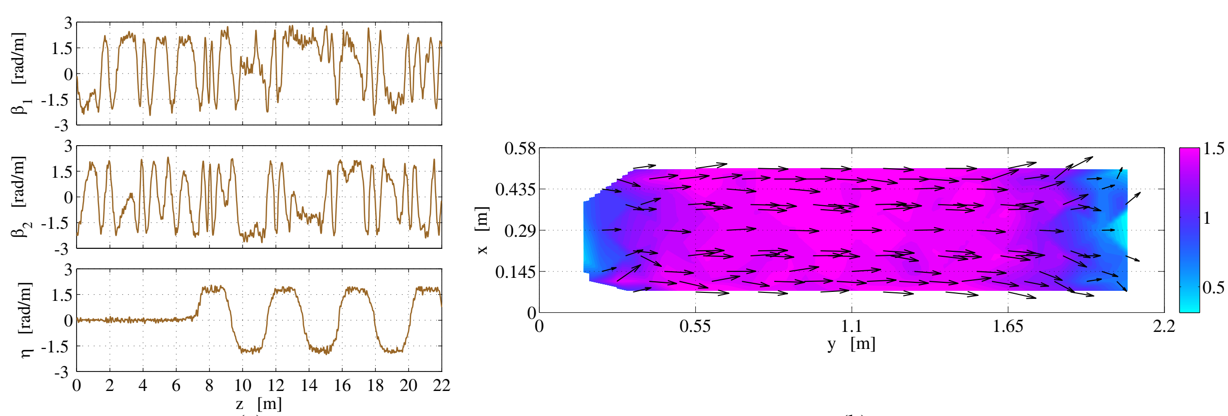

(a) (b)

Figure 2: (a) Components of $\boldsymbol{\beta}(z)$ measured along fiber path I of sensor A. (b) 2D vectorial map of magnetic field in the MRI scanner.

Along the board axis, at $x = 0.29$ m, the fibers create nine crossing where the magnetic field can be measured along three different directions. These points offer the opportunity to estimate the uncertainty of the magnetic field measure, which is about 7%. Furthermore, the limit of detection of the sensor is around 100 mT, as evaluated from the fiber sections not exposed to the magnetic field. We remark, however, that these measurements have been performed by using standard G.652 telecommunication fibers.

4. 3D VECTORIAL MEASUREMENT OF MAGNETIC FIELD

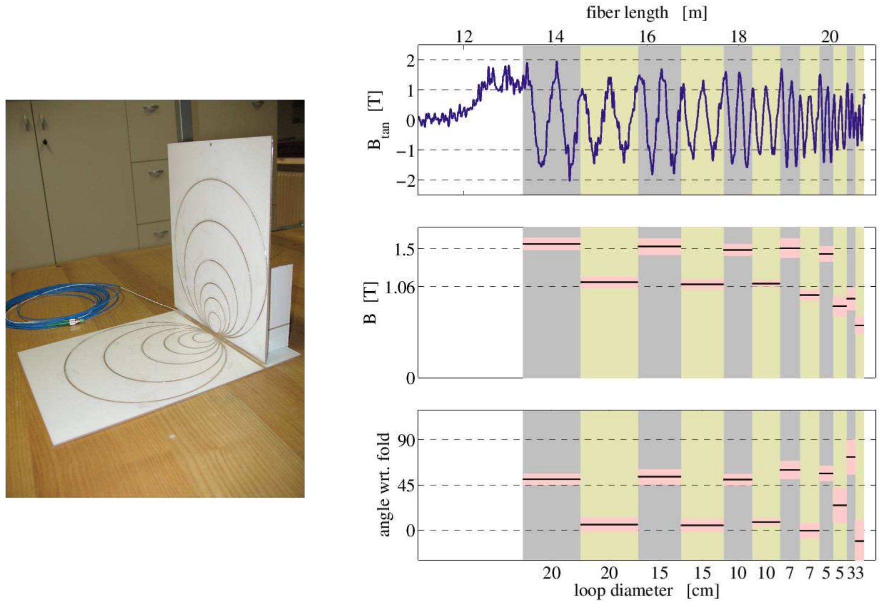

(a) (b)

Figure 3: (a) Layout of the 3D magnetic field sensor B. (b) Measurements taken on the sensor when oriented at 45° with respect to the magnetic field.

The principle exposed in the previous section can be generalized to perform 3-dimensional vectorial measurements, provided that the fiber is arranged so to span the 3 dimensions. As a proof of concept, we have implemented the sensor "B" shown in Fig. 3(a), where the basic idea is to have the fiber wound on loops on two orthogonal plates [7]. We assume that the magnetic field is constant in the volume of the sensor; this sets the spatial resolution of the sensor. We also use the "fold axis", i.e., the axis along which the loop plates are in contact, as a reference. All loops are, by construction, tangent to the fold axis.

Let consider first the effect of a single loop. Since the magnetic field is constant, the angle $\psi(z)$ in (2) varies sinusoidally along the fiber of the loop. Therefore, we can express the Faraday rotation along the fiber loop as

$$\eta(z) = 2VB_{\text{plane}} \cos(2\pi z/L_{\text{loop}} + \phi_0)\,, \tag{3}$$

where B_{plane} is the intensity of the magnetic induction component projected on to the loop plane and L_{loop} is the loop length. If we set $z = 0$ at the point where the loop is tangent to the fold axis, we can say that ϕ_0 is the angle subtended by the magnetic field projection on the loop plane and the fold axis. So if these two are, for example, anti-parallel, then $\phi_0 = \pi$.

According to the above model, by performing a Fourier analysis of the measured Faraday rotation $\eta(z)$ and considering only the signal at the known spatial frequency given by the loop length, we can extract the intensity B_{plane} of the magnetic induction projection on the loop plane and its orientation ϕ_0 with respect to the fold axis. Finally, repeating the measurement on an orthogonal plane we have a complete 3-dimensional measurement of the magnetic induction.

The sensor we implemented had several circular paths with diameters of 3, 5, 7, 10, 15 and 20 cm. This was done to determine the best achievable spatial resolution and, at the same time, to prove that many of these sensors can be concatenated. Each path hosts two loops of fiber; the fiber enters the sensor along the fold axis, and goes twice along each loop, starting from the larger ones, and alternating horizontal and vertical planes. The results of the measurement performed in the same MRI scanner of Fig. 1(c) are shown in Fig. 3(b). The sensor was oriented in such a way that the magnetic induction was parallel to the horizontal plane, and at 45° with respect to the vertical one and to the fold axis. The top graph shows $\eta(z)/(2V)$, which is the intensity of the magnetic induction component tangent to the fiber at each point z. Gray (yellow) background refers to fiber sections on the horizontal (vertical) planes. We clearly see the oscillation described by (3), and a closer look reveals also the change of amplitude and phase between vertical and horizontal planes. Despite the raw data is noisy, the Fourier analysis extracts B_{plane} and ϕ_0 quite accurately.

These are shown in the middle and lower graphs, respectively, where the solid black line indicate the calculated values and the pink band their uncertainties. While at lower loop diameters the measurement is not accurate due to the limited spatial resolution of the POFDR, for diameters of 10 cm or above results are in good agreement with the nominal ones, marked by the dashed lines.

5. CONCLUSION

In this paper we have reviewed the recent achievements on distributed measurements of intense magnetic fields. This new class of distributed sensors is based on polarization reflectometry and on a novel data analysis algorithm, that allows to single Faraday rotation out of the random variations of the backscattered polarization. Two different sensors have been described. The first one enables the 2-dimensional vectorial mapping of the magnetic field with a spatial resolution in the order of few centimeters; as an example, the field of an MRI scanner for medical applications has been successfully mapped. The second sensors enables the 3-dimensional vectorial measurement of magnetic field at specific position, with resolution in the order of 10 cm. Owing to its distributed nature, this sensor can be easily concatenated to have a multi-point sensor. Despite limited to strong magnetic field due to the small Verdet constant of silica fibers, this new class of distributed magnetic field optical fiber sensors paves the way to unprecedented applications, such as distributed current measurements.

REFERENCES

1. Grattam, K. T. V. and B. T. Maggitt, *Optical Fiber Sensor Technology,* Kluwer Academic Publishers, Dordrecht, 2000.
2. Rashleigh, S. C., "Magnetic-field sensing with a single-mode fiber," *Opt. Lett.*, Vol. 6, No. 1, 19–21, 1981.
3. Annovazzi-Lodi, V., S. Donati, and S. Merlo, "Coiled-fiber sensor for vectorial measurement of magnetic field," *J. Lightw. Technol.*, Vol. 10, No. 12, 2006–2010, 1992.
4. Palmieri, L. and A. Galtarossa, "Distributed polarization-sensitive reflectometry in nonreciprocal single-mode optical fibers," *J. Lightwave Technol.*, Vol. 29, No. 21, 3178–3184, 2011.
5. Palmieri, L. and A. Galtarossa, "Distributed fiber optic sensor for mapping of intense magnetic fields based on polarization sensitive reflectometry," *Proc. SPIE*, Vol. 8351, 2012.
6. Palmieri, L., "Distributed polarimetric measurements for optical fiber sensing," *Optical Fiber Technology*, Vol. 19, No. 6, Part B, 720–728, 2013.
7. Palmieri, L., E. Autizi, and A. Galtarossa, "A novel quasi-distributed fiber optic sensor for 3D vector measurement of static magnetic fields," *Proc. SPIE*, Vol. 8794, 2013.
8. Ross, J. N., "Measurement of magnetic field by polarisation optical time-domain reflectometry," *Electron. Lett.*, Vol. 17, No. 17, 596–597, 1981.
9. Wuilpart, M., C. Caucheteur, A. Goussarov, M. Aerssens, V. Massaut, and P. Megret, "Measurement of magnetic field using Rayleigh backscattering in optical fibres," *ANIMMA 2011*, 1–6, 2011.
10. Aerssens, M., A. Gusarov, P. Moreau, P. Malard, V. Massaut, P. Mégret, and M. Wuilpart, "Development of a Jones vector based model for the measurement of a plasma current in a thermonuclear fusion reactor with a POTDR setup," *Proc. SPIE*, Vol. 8439, 2012.
11. Rashleigh, S., "Origins and control of polarization effects in single-mode fibers," *Journal of Lightwave Technology*, Vol. 1, 312–331, 1983.
12. Rogers, A. J., "Polarization-optical time domain reflectometry: A technique for the measurement of field distributions," *Appl. Opt.*, Vol. 20, 1060–1074, 1981.
13. Palmieri, L. and L. Schenato, "Distributed optical fiber sensing based on Rayleigh scattering," *The Open Optics Journal*, Vol. 7, Special Issue 1, 104–127, 2013.
14. Jopson, R., L. Nelson, and H. Kogelnik, "Measurement of second-order polarization-mode dispersion vectors in optical fibers," *IEEE Photon. Technol. Lett.*, Vol. 11, No. 9, 1153–1155, 1999.
15. Someda, C. G., *Electromagnetic Waves*, CRC/Taylor & Francis, Boca Raton, FL, 2006.
16. Noda, J., T. Hosaka, Y. Sasaki, and R. Ulrich, "Dispersion of verdet constant in stress-birefringent silica fibre," *Electron. Lett.*, Vol. 20, No. 22, 906–908, 1984.